Contents lists available at ScienceDirect

Physics Letters B

Constraints on the neutrino emission from the Galactic Ridge with the ANTARES telescope

S. Adrián-Martínez [a], A. Albert [b], M. André [c], M. Anghinolfi [ab], G. Anton [d], M. Ardid [a], J.-J. Aubert [e], T. Avgitas [f], B. Baret [f], J. Barrios-Martí [g], S. Basa [h], V. Bertin [e], S. Biagi [i], R. Bormuth [j,k], M.C. Bouwhuis [j], R. Bruijn [j,l], J. Brunner [e], J. Busto [e], A. Capone [m,n], L. Caramete [o], J. Carr [e], S. Celli [m,n], T. Chiarusi [p], M. Circella [q], A. Coleiro [f], R. Coniglione [i], H. Costantini [e], P. Coyle [e], A. Creusot [f], A. Deschamps [r], G. De Bonis [m,n], C. Distefano [i], C. Donzaud [f,s], D. Dornic [e], D. Drouhin [b], T. Eberl [d], I. El Bojaddaini [t], D. Elsässer [u], A. Enzenhöfer [d], K. Fehn [d], I. Felis [a], L.A. Fusco [p,v,*], S. Galatà [f], P. Gay [w,f], S. Geißelsöder [d], K. Geyer [d], V. Giordano [x], A. Gleixner [d], H. Glotin [y,z], R. Gracia-Ruiz [f], K. Graf [d], S. Hallmann [d], H. van Haren [aa], A.J. Heijboer [j], Y. Hello [r], J.J. Hernández-Rey [g], J. Hößl [d], J. Hofestädt [d], C. Hugon [ab,ac], G. Illuminati [m,n], C.W. James [d], M. de Jong [j,k], M. Kadler [u], O. Kalekin [d], U. Katz [d], D. Kießling [d], A. Kouchner [f,z], M. Kreter [u], I. Kreykenbohm [ad], V. Kulikovskiy [i,ae], C. Lachaud [f], R. Lahmann [d], D. Lefèvre [af], E. Leonora [x,ag], S. Loucatos [ah,f], M. Marcelin [h], A. Margiotta [p,v], A. Marinelli [ai,aj], J.A. Martínez-Mora [a], A. Mathieu [e], T. Michael [j], P. Migliozzi [ak], A. Moussa [t], C. Mueller [u], E. Nezri [h], G.E. Păvălaş [o], C. Pellegrino [p,v], C. Perrina [m,n], P. Piattelli [i], V. Popa [o], T. Pradier [al], C. Racca [b], G. Riccobene [i], K. Roensch [d], M. Saldaña [a], D.F.E. Samtleben [j,k], A. Sánchez-Losa [g,q], M. Sanguineti [ab,ac], P. Sapienza [i], J. Schnabel [d], F. Schüssler [ah], T. Seitz [d], C. Sieger [d], M. Spurio [p,v], Th. Stolarczyk [ah], M. Taiuti [ab,ac], A. Trovato [i], M. Tselengidou [d], D. Turpin [e], C. Tönnis [g], B. Vallage [ah,f], C. Vallée [e], V. Van Elewyck [f], E. Visser [j], D. Vivolo [ak,am], S. Wagner [d], J. Wilms [ad], J.D. Zornoza [g], J. Zúñiga [g]

[a] Institut d'Investigació per a la Gestió Integrada de les Zones Costaneres (IGIC) – Universitat Politècnica de València, C/ Paranimf 1, 46730 Gandia, Spain
[b] GRPHE – Université de Haute Alsace – Institut universitaire de technologie de Colmar, 34 rue du Grillenbreit, BP 50568 – 68008 Colmar, France
[c] Technical University of Catalonia, Laboratory of Applied Bioacoustics, Rambla Exposició, 08800 Vilanova i la Geltrú, Barcelona, Spain
[d] Friedrich–Alexander-Universität Erlangen–Nürnberg, Erlangen Centre for Astroparticle Physics, Erwin-Rommel-Str. 1, 91058 Erlangen, Germany
[e] Aix-Marseille Université, CNRS/IN2P3, CPPM UMR 7346, 13288 Marseille, France
[f] APC, Université Paris Diderot, CNRS/IN2P3, CEA/IRFU, Observatoire de Paris, Sorbonne Paris Cité, 75205 Paris, France
[g] IFIC – Instituto de Física Corpuscular, c/ Catedráatico José Beltrán, 2, E-46980 Paterna, Valencia, Spain
[h] LAM – Laboratoire d'Astrophysique de Marseille, Pôle de l'Étoile Site de Château-Gombert, rue Frédéric Joliot-Curie 38, 13388 Marseille Cedex 13, France
[i] INFN – Laboratori Nazionali del Sud (LNS), Via S. Sofia 62, 95123 Catania, Italy
[j] Nikhef, Science Park, Amsterdam, The Netherlands
[k] Huygens–Kamerlingh Onnes Laboratorium, Universiteit Leiden, The Netherlands
[l] Universiteit van Amsterdam, Instituut voor Hoge-Energie Fysica, Science Park 105, 1098 XG Amsterdam, The Netherlands
[m] INFN – Sezione di Roma, P.le Aldo Moro 2, 00185 Roma, Italy
[n] Dipartimento di Fisica dell'Università La Sapienza, P.le Aldo Moro 2, 00185 Roma, Italy
[o] Institute for Space Science, RO-077125 Bucharest, Măgurele, Romania
[p] INFN – Sezione di Bologna, Viale Berti-Pichat 6/2, 40127 Bologna, Italy
[q] INFN – Sezione di Bari, Via E. Orabona 4, 70126 Bari, Italy
[r] Géoazur, UCA, CNRS, IRD, Observatoire de la Côte d'Azur, Sophia Antipolis, France
[s] Univ. Paris-Sud, 91405 Orsay Cedex, France
[t] University Mohammed I, Laboratory of Physics of Matter and Radiations, B.P.717, Oujda 6000, Morocco
[u] Institut für Theoretische Physik und Astrophysik, Universität Würzburg, Emil-Fischer Str. 31, 97074 Würzburg, Germany
[v] Dipartimento di Fisica e Astronomia dell'Università, Viale Berti Pichat 6/2, 40127 Bologna, Italy

* Corresponding author at: INFN – Sezione di Bologna and Dipartimento di Fisica e Astronomia dell'Università di Bologna, Viale Berti-Pichat 6/2, 40127 Bologna, Italy.
E-mail address: luigiantonio.fusco@bo.infn.it (L.A. Fusco).

[w] *Laboratoire de Physique Corpusculaire, Clermont Univertsité, Université Blaise Pascal, CNRS/IN2P3, BP 10448, F-63000 Clermont-Ferrand, France*
[x] *INFN – Sezione di Catania, Viale Andrea Doria 6, 95125 Catania, Italy*
[y] *LSIS, Aix Marseille Université, CNRS, ENSAM, LSIS, UMR 7296, 13397 Marseille, France; Université de Toulon, CNRS, LSIS, UMR 7296, 83957 La Garde, France*
[z] *Institut Universitaire de France, 75005 Paris, France*
[aa] *Royal Netherlands Institute for Sea Research (NIOZ), Landsdiep 4, 1797 SZ 't Horntje (Texel), The Netherlands*
[ab] *INFN – Sezione di Genova, Via Dodecaneso 33, 16146 Genova, Italy*
[ac] *Dipartimento di Fisica dell'Università, Via Dodecaneso 33, 16146 Genova, Italy*
[ad] *Dr. Remeis-Sternwarte and ECAP, Universität Erlangen–Nürnberg, Sternwartstr. 7, 96049 Bamberg, Germany*
[ae] *Moscow State University, Skobeltsyn Institute of Nuclear Physics, Leninskie Gory, 119991 Moscow, Russia*
[af] *Mediterranean Institute of Oceanography (MIO), Aix-Marseille University, 13288, Marseille Cedex 9, France; Université du Sud Toulon-Var, 83957, La Garde Cedex, France CNRS-INSU/IRD UM 110*
[ag] *Dipartimento di Fisica ed Astronomia dell'Università, Viale Andrea Doria 6, 95125 Catania, Italy*
[ah] *Direction des Sciences de la Matière – Institut de recherche sur les lois fondamentales de l'Univers – Service de Physique des Particules, CEA Saclay, 91191 Gif-sur-Yvette Cedex, France*
[ai] *INFN – Sezione di Pisa, Largo B. Pontecorvo 3, 56127 Pisa, Italy*
[aj] *Dipartimento di Fisica dell'Università, Largo B. Pontecorvo 3, 56127 Pisa, Italy*
[ak] *INFN – Sezione di Napoli, Via Cintia, 80126 Napoli, Italy*
[al] *Université de Strasbourg, IPHC, 23 rue du Loess, 67037 Strasbourg, France – CNRS, UMR7178, 67037 Strasbourg, France*
[am] *Dipartimento di Fisica dell'Università Federico II di Napoli, Via Cintia, 80126 Napoli, Italy*

ARTICLE INFO

ABSTRACT

A highly significant excess of high-energy astrophysical neutrinos has been reported by the IceCube Collaboration. Some features of the energy and declination distributions of IceCube events hint at a North/South asymmetry of the neutrino flux. This could be due to the presence of the bulk of our Galaxy in the Southern hemisphere. The ANTARES neutrino telescope, located in the Mediterranean Sea, has been taking data since 2007. It offers the best sensitivity to muon neutrinos produced by galactic cosmic ray interactions in this region of the sky. In this letter a search for an extended neutrino flux from the Galactic Ridge region is presented. Different models of neutrino production by cosmic ray propagation are tested. No excess of events is observed and upper limits for different neutrino flux spectral indices Γ are set. For $\Gamma = 2.4$ the 90% confidence level flux upper limit at 100 TeV for one neutrino flavour corresponds to $\Phi_0^{1f}(100 \text{ TeV}) = 2.0 \cdot 10^{-17} \text{ GeV}^{-1} \text{ cm}^{-2} \text{ s}^{-1} \text{ sr}^{-1}$. Under this assumption, at most two events of the IceCube cosmic candidates can originate from the Galactic Ridge. A simple power-law extrapolation of the Fermi-LAT flux to account for IceCube High Energy Starting Events is excluded at 90% confidence level.

1. Introduction

Neutrino telescopes search for high-energy ($E_\nu \gg$ GeV) neutrinos produced by astrophysical objects. The ANTARES detector [1] is the largest underwater neutrino telescope. Its effective area, good angular resolution and good exposure to the southern sky has allowed the detector to produce the best limits on neutrino emission up to 100 TeV from point-like objects at negative declinations [2].

The IceCube Collaboration has reported the observation of astrophysical neutrinos with the High Energy Starting Events (HESE) [3,4], and confirmed the discovery in other analyses [5,6]. The selection of HESE and of the lower-energy events reported in [5] is based on vetoing techniques [7], detecting contained events from all directions, and the observed signal is dominantly composed of shower-type events. Individual neutrino sources have not been identified so far. The flux of these events is compatible with the hypothesis of isotropy [8] and equipartition in the three neutrino flavours [9]. The limited statistic and the poor angular resolution make the HESE sample insensitive to a possible asymmetry from neutrinos arising from the northern and southern sky regions.

Muon neutrinos coming from the northern hemisphere are detected as upward-going muon tracks. The IceCube Collaboration has observed astrophysical neutrinos also in this upward-going sample [6]. By comparing the spectral energy distribution of this sample to that of other analyses, a difference in the shape between the neutrino flux observed in the southern sky and the one from the northern sky is found, with a significance of 2σ.

For the ANTARES location, in the Mediterranean Sea, the southern sky is accessible via upward-going muon tracks, for which a median angular resolution of $0.4°$ for a E_μ^{-2} neutrino energy spectrum is achieved [10]. Individual neutrino sources have been searched for using ANTARES data alone [2] and in combination with IceCube events [11]. The search method uses an unbinned maximum likelihood ratio estimation that accounts for the energy and directional information of individual neutrino candidates. This significantly reduces the influence of the atmospheric background in the search for a cosmic signal.

The current ANTARES upper limit on point-like sources in the central region of the Galaxy corresponds to a spectral energy distribution $E_\nu^2 dN_\nu/dE_\nu \sim 0.9 \cdot 10^{-8} \text{ GeV cm}^{-2} \text{ s}^{-1}$. At 1 TeV, this limit is about four times higher than the neutrino flux expected by the only hadronic accelerator discovered so far in our Galaxy [12]. However, as motivated in §2, the Galactic plane is considered a guaranteed extended source of neutrinos originating from the decay of short-lived particles induced by the interaction of cosmic rays (CRs) with interstellar matter. Recent computations [13, 14] suggest that the neutrino yield from this process could be at least one order of magnitude larger than that of still unresolved point-like sources. These conclusions have been derived by the measurement of the flux of γ-rays by satellite and ground experiments, part of which is due to hadronic mechanisms than produce neutrinos as well. This neutrino flux is anyway too low to entirely explain the IceCube signal observed in the Southern sky [15,16].

In this letter, a search for neutrinos ($\nu_\mu + \bar{\nu}_\mu$) on an extended region of solid angle $\Delta\Omega = 0.145$ sr centred in the Galactic ori-

gin is described. Data collected by the ANTARES neutrino telescope (described in §3) from 2007 to 2013 have been used. Atmospheric neutrinos represent a diffuse, irreducible background for all searches of neutrinos of astrophysical origin. The flux of atmospheric neutrino at 1 TeV is more than three order of magnitude larger than the signal reported in [5]. Differently from the search of neutrino point-like sources, the method considered here relies on the search for an excess of neutrino-induced upward going events in the high-energy tail of the measured spectrum. The observed muon provides a proxy of the neutrino energy [17]. The signal is in fact expected with harder spectral index ($\propto E_\nu^{-\Gamma}$, with Γ studied from 2.0 to 2.7) with respect to that of the background ($\propto E_\nu^{-3.7}$). A crucial point to maximise the signal is the definition of the size of the considered region. The challenges of this work in the reduction of the background and the optimisation procedures based on Monte Carlo simulations are described in §4. The results of the analysis are presented and discussed in §5 and §6.

2. Neutrinos from our Galaxy and the IceCube signal

The isotropic flux of high-energy cosmic neutrinos measured by the IceCube Collaboration was modelled with power-laws $dN_\nu/dE_\nu = \Phi_0 E_\nu^{-\Gamma}$, yielding relatively soft spectral indices ($\Gamma > 2$). The value $\Gamma = 2$ is expected for neutrinos produced from primary CRs accelerated by the simplest Fermi shock acceleration models [19,20] and interacting near their sources [21]. The $E_\nu^{-2.0}$ spectrum is excluded [8] in the energy range between 25 TeV and 2.8 PeV with a significance of more than 3.8σ, assuming that the astrophysical neutrino flux is isotropic and consisting of equal flavours at Earth. Under the same assumptions, the best-fit spectral index is $\Gamma = 2.50 \pm 0.09$ and the normalisation at the energy of 100 TeV (for all three neutrino flavours, $3f$) is $\Phi_0^{3f}(100\ \mathrm{TeV}) = 6.7^{+1.1}_{-1.2} \cdot 10^{-18}\ \mathrm{GeV}^{-1}\ \mathrm{cm}^{-2}\ \mathrm{s}^{-1}\ \mathrm{sr}^{-1}$. No significant excess is found when searching for spatial anisotropies. Muon neutrinos coming from the northern hemisphere [6] yields a best-fit, single-flavour flux $\Phi_0^{1f}(100\ \mathrm{TeV}) = 9.9^{+3.9}_{-3.4} \cdot 10^{-19}\ \mathrm{GeV}^{-1}\ \mathrm{cm}^{-2}\ \mathrm{s}^{-1}\ \mathrm{sr}^{-1}$ and assuming $\Gamma = 2$. It is worth noting that this particular channel can access neutrinos only at energies above 100 TeV because of the more abundant atmospheric background from ν_μ-induced events, while analyses including shower-like neutrino interactions have lower energy thresholds.

The separate fit of the fluxes from the northern and southern hemispheres [8] indicates a preference (although with small statistical significance) for a harder spectrum in the northern hemisphere. Moreover, some authors have observed that events are concentrated near the Galactic Centre and Galactic Plane regions in a way that seems inconsistent with an isotropic neutrino distribution [22,23]. Such a difference between the northern and southern skies could potentially stem from the presence of a softer contribution to the neutrino flux from the Galaxy in the southern hemisphere [24].

The isotropic distribution of extragalactic sources (such as active galactic nuclei or γ-ray bursts) presumably dominates the signal from the northern hemisphere. Models generally predict that neutrinos from these sources will be generated via photo-hadronic interactions of high-energy protons with low-energy photons of the background. These models are characterised by relatively high-energy thresholds (due to charged pion production) and disfavour a soft neutrino spectrum [25,26]. Other extragalactic sources, such as starburst galaxies [27], are expected to produce neutrinos primarily by proton–proton (or nuclei) interactions and subsequent decay of secondary charged mesons (mainly pions). In this case, the emission has a spectral index Γ close to that of the parent hadrons and a lower energy threshold [28]. Since in p–p interactions the number of charged pions is approximately twice that of

neutral pions (which decay to a pair of γ), the neutrino flux can be constrained from the observed γ-ray flux. Due to the high density of matter in the central part of the Galactic Plane, a neutrino signal coming from this part of the sky, mostly located in the southern hemisphere, is expected to follow this emission scenario.

Fermi-LAT data provide the best measurement of the diffuse γ-ray flux in the Galactic Plane up to ~ 100 GeV [29]. Given certain model assumptions, the fraction of this flux attributed to hadronic processes can be estimated, allowing the derivation of the neutrino yield from CR propagation. Models with a constant diffusion coefficient of CR in our Galaxy predict a much lower and softer neutrino spectrum ($\Gamma \simeq 2.7$) [30,31] than that measured by IceCube.

New predictions for the neutrino production due to CR propagation have been presented recently. The authors of [13] start with the observation that conventional models of Galactic CR propagation cannot explain the large γ-ray flux measured by Milagro [32] from the inner Galactic Plane region and by H.E.S.S. [33] from the Galactic Ridge region. To reconcile *Fermi*-LAT, Milagro and H.E.S.S. data, they have developed a phenomenological model characterised by radially-dependent CR transport properties, which predicts a neutrino spectral index in the range $\Gamma \simeq 2.4$–2.5. In [14], a sizeable neutrino flux is expected to be produced by the interaction of fresh CRs, which are hadrons supplied by young accelerators and contained by the local magnetic field, with the ambient matter. The authors of [34] note that IceCube observes 3 events in the $E_\nu > 100$ TeV energy range with arrival direction compatible with a Galactic Ridge origin ($|\ell| < 30°$, $|b| < 4°$). Furthermore, the corresponding neutrino flux matches the high-energy power-law extrapolation of the spectrum of diffuse γ-ray emission from the Galactic Ridge as observed by *Fermi*-LAT. This motivates the hypothesis that these IceCube neutrino events and *Fermi*-LAT γ-ray flux are both produced in interactions of CRs with the interstellar medium in the inner Galactic region. All these models predict an enhancement of the neutrino flux coming from a limited region close to the Galactic Centre.

3. The ANTARES detector and dataset

The ANTARES underwater neutrino telescope [1] is located 40 km off the southern coast of France in the Mediterranean Sea (42° 48′ N, 6° 10′ E). It consists of a three-dimensional array of 10-inch photomultiplier tubes (PMTs). Neutrino detection is based on the observation of Cherenkov light induced in the medium by relativistic charged particles. Some of the emitted photons produce signals in the PMTs ("hits"). The position, time and collected charge of the hits are used to infer the direction and energy of the incident neutrino.

The study presented here focuses on track-like events, associated with CC interactions of muon neutrinos. The muon direction is correlated with that of the incoming neutrino, and a sub-degree angular resolution on the neutrino arrival direction can be achieved by means of a maximum likelihood fit [10].

Data collected from May 2007 to December 2013 constitute the data sample for the present analysis, with an effective total lifetime of 1622 days. High quality data runs, defined according to environmental and data taking conditions, have been selected for this work (analogously to [2]). A detailed Monte Carlo simulation is available for each data acquisition run [35,36].

4. The search method

An enhancement of the neutrino diffuse emission from a region of the sky covering a small solid angle can be searched for

by comparing the number of events coming from the region (on-zone) to that of regions with no expected signal and the same acceptance to the background (off-zones). To enhance the harder signal over the background of atmospheric neutrinos, a cut selecting mainly high-energy events is defined. This approach has already been used to search for neutrino candidates from the region of the Fermi Bubbles [37]. Optimising this method requires: 1) an efficient suppression of atmospheric events; 2) the optimisation of the size of the search region and 3) the subsequent definition of background-only regions, each having the same exposure as that of the signal region. The analysis uses Monte Carlo simulations only in the optimisation of the event selection; this avoids biases in the estimation of the signal and background and reduces systematic effects. Monte Carlo data sets are produced simulating real data acquisition conditions, taking into account the actual detection efficiency of the apparatus.

The signal is assumed to be a power-law diffuse flux with arbitrary normalisation and spectral indices varying from $\Gamma = 2.0$ to 2.7. Motivated by the IceCube best fit and models of neutrino production from CR propagation, the event selection criteria have been optimised in order to achieve the best sensitivity for a signal with spectral index $\Gamma = 2.4$. They are identical to those obtained for $\Gamma = 2.5$. The optimal cuts are found using the Model Rejection Factor (MRF) minimisation technique [38].

The background component due to mis-reconstructed atmospheric muons, which mimick upgoing neutrino events, has been simulated using the MUPAGE program [39]. This background is suppressed by cuts on quality parameters of upgoing reconstructed tracks: Λ, which is related to the maximum likelihood of the fit, and β, which estimates the angular error. The distributions of Λ and β for atmospheric neutrinos, atmospheric muons and data are reported in [10]. It is found that the cut $\Lambda > -5.0$ and $\beta < 0.5°$ optimises the MRF and suppresses the contamination from wrongly reconstructed atmospheric muons in the upgoing sample to the level of 1%.

The remaining background consists of atmospheric neutrinos [17]. The *conventional* component, coming from the decay of pions and kaons, has been modelled according to [40] while the flux from [41] has been used for the *prompt* component, expected from charmed hadron decays. This component is reduced by imposing a cut on the estimated energy of the events, limiting the event sample to the energy where the harder cosmic flux is expected to emerge above the atmospheric background. For this analysis, the energy estimator E_{ANN} [18], derived from an artificial neural network algorithm, is used. The standard deviation of the variable $\log_{10}(E_{ANN}/E_{true})$, where E_{true} is the Monte Carlo true energy of the muon, is almost constant at ~ 0.4 over the considered energy range. The MRF optimisation results in $E_{ANN}^{cut} = 10$ TeV as the best cut value. Above E_{ANN}^{cut}, only 6% of the selected atmospheric neutrinos survive while 40% of the signal (for $\Gamma = 2.4$) passes the cut.

Assuming a direct connection between the emission of γ-rays and neutrinos from pion decay in hadronic mechanisms [42], the γ-ray flux measured by *Fermi*-LAT [29] is used to estimate the flux of Galactic neutrinos. Though this diffuse emission is extended over the whole Galactic Plane, it is much brighter in the very central region; including non-central regions of the plane in this search would mostly increase the atmospheric background. The MRF method is used to determine the optimal search region for each spectral index. For a signal spectrum with $\Gamma = 2.4$, the signal region is represented by the rectangle (enclosing the Galactic Centre) in galactic coordinates with longitude $|\ell| < 40°$ and latitude $|b| < 3°$. This corresponds to a solid angle of $\Delta\Omega = 0.145$ sr. Modifications to the longitudinal size of the signal region do not significantly reduce the resulting sensitivity, while the latitude bound
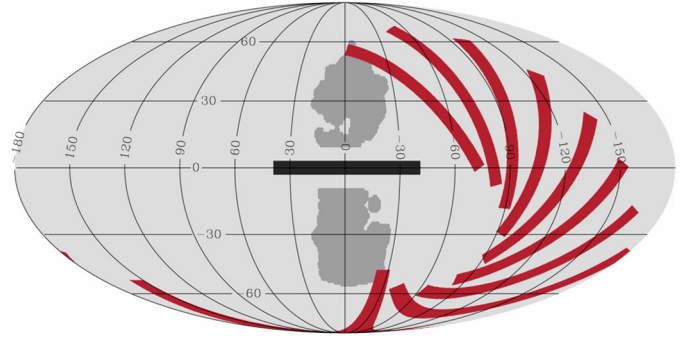
Fig. 1. Aitoff projection in galactic coordinates of the signal (black) and background (red) regions, representing the considered Galactic Plane region and off-zones of the analysis. Also shown are the Fermi Bubbles (grey) as in [43]. The signal region, delimited by $|\ell| < 40°$, $|b| < 3°$ covers a solid angle of 0.145 sr. (For interpretation of the references to colour in this figure legend, the reader is referred to the web version of this article.)

has a larger effect – about 10% worsening per degree of increased size.

Off-zones are defined as fixed regions in equatorial coordinates, which have identical size and shape as the signal region and are not overlapping with it or each other. In local coordinates, off-zones span the same fraction of the sky as the on-zone, but with some fixed delay in time, i.e. they differ only in right ascension. They are shifted in the sky to avoid any overlap with the Fermi Bubble regions [43], so that none of the possible signal events from these areas enters into the background estimation. The maximum number of independent off-zone regions is 9. The signal and background regions in galactic coordinates are shown in Fig. 1. Data from the signal region were blinded until the event selection procedure was completely defined. Off-zones can also be used to test the agreement between data and Monte Carlo.

After the optimisation procedure, considering a signal flux with an energy spectrum with $\Gamma = 2.4$ (2.5) the expected limit at 90% confidence level (c.l.) for the considered data sample corresponds to $\Phi_0^{1f}(1 \text{ GeV}) = 2.0$ (6.0) $\cdot 10^{-5}$ GeV^{-1} cm^{-2} s^{-1} sr^{-1}. For the normalisation at a different energy E, the fluxes must be multiplied by the factor $\left(\frac{E}{1 \text{ GeV}}\right)^{-\Gamma}$. For all flavours, the normalisation must be multiplied by a factor three under the assumption of a cosmic flux in flavour equipartition ($\nu_e : \nu_\mu : \nu_\tau = 1 : 1 : 1$). The energy range between 3 and 300 TeV contains the central 90% of the expected detected signal.

5. Results

After the unblinding of the entire data sample, 3.7 events surviving cuts are observed on average in the off-zone regions, while two are detected from the Galactic Plane region. In the evaluation of the upper limit, our method is sensitive only to signals in excess of the off-zones, i.e. any isotropic flux is treated as background for this purpose. The isotropic neutrino flux of astrophysical origin as measured by IceCube would produce 0.2 events equivalently in each off-zone and in the on-zone region. The distributions of the number of selected events in the on-zone and off-zone regions as a function of the reconstructed energy are reported in Fig. 2.

A smaller number of events is observed in the signal region than the expected background, and the Feldman and Cousins 90% c.l. upper bound [44] is computed. For $\Gamma = 2.4$ the corresponding flux $\Phi_0^{1f}(1 \text{ GeV}) = 1.5 \cdot 10^{-5}$ GeV^{-1} cm^{-2} s^{-1} sr^{-1}. However, adopting the same conservative approach as for the limits from selected point-like sources [2] in the case of an underfluctuation, the 90% c.l. upper limit on the signal flux is set to the value of the
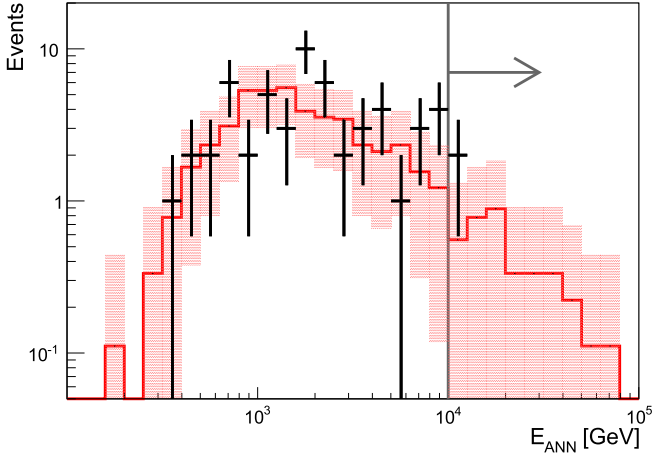
Fig. 2. Distribution of the reconstructed energy E_{ANN} of upgoing muons in the Galactic Plane (black crosses) and average of the off-zone regions (red histogram). The grey line shows the energy selection cut applied in the procedure.
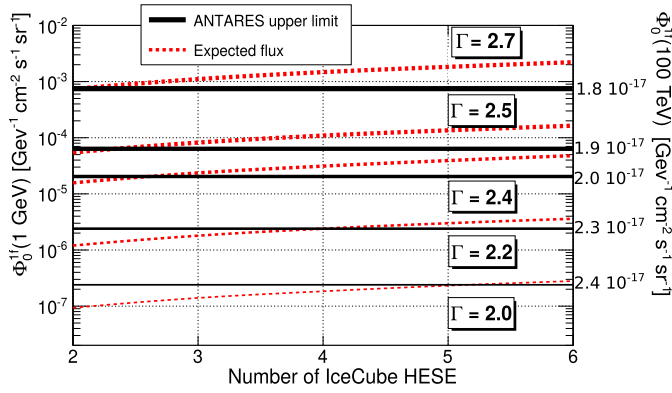

Fig. 3. ANTARES upper limits (black) derived for the Galactic Plane region for different signal spectral indices Γ, compared to the flux required to produce from 2 to 6 IceCube HESE in the signal region (red dashed lines). Selection cuts have been optimised for $\Gamma = 2.4$ and 2.5. The limits for softer and harder spectral indices are thus derived with non-optimal criteria. The values of the normalisation factor Φ_0^{1f} (100 TeV) are reported on the right y-axis.

ANTARES sensitivity. One limit for each considered spectral index is obtained.

The 90% c.l. upper limits on Φ_0^{1f} (1 GeV) are reported in Fig. 3 for particular values of Γ. For each value of Γ, the one-flavour neutrino flux from the considered region necessary to produce from 2 to 6 HESE is also reported. The curves are computed on the basis of the effective areas reported in [3] according to the prescription of [24]. All fluxes above the horizontal black lines are excluded at 90% c.l. by ANTARES observation. For instance, a flux with spectral index $\Gamma = 2.5$ that produces 3 or more HESE in the signal region of $\Delta\Omega = 0.145$ sr is excluded. For the conventional CR propagation scenario, the 90% c.l. upper limit for $\Gamma = 2.7$ is Φ_0^{1f} (1 GeV) $= 7.5 \cdot 10^{-4}$ GeV^{-1} cm^{-2} s^{-1} sr^{-1}.

Fig. 4 shows the computed ANTARES 90% c.l. upper limit for the neutrino emission in the region $|\ell| < 40°$ and $|b| < 3°$ assuming a $\Gamma = 2.4$ neutrino flux. The limit on Φ_0^{3f} assuming flavour equipartition is reported, along with expectations from models. The simple extrapolation [34] to IceCube energies of the diffuse γ-ray flux measured by *Fermi*-LAT [29] is excluded at 90% confidence level, assuming flavour equipartition. Models (KRA$_\gamma$, Fig. 4) that consider a harder CR spectrum in the inner Galaxy, and the hardening of the CR spectrum measured by PAMELA and AMS-02 [13], yield a neutrino flux (at 100 TeV) of a factor of two to three lower. Models
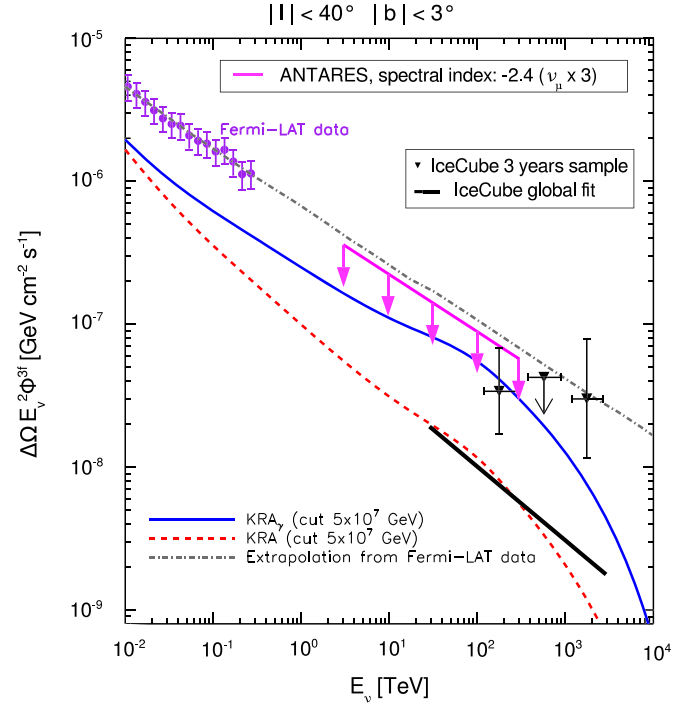
Fig. 4. ANTARES upper limit (magenta line) on the neutrino flux integrated over the solid angle $\Delta\Omega = 0.145$ sr corresponding to the Galactic Plane region $|\ell| < 40°$, $|b| < 3°$. Our limit is compared to expectations as computed in [13], assuming a CR cut-off at 5×10^7 GeV, both with (KRA$_\gamma$) and without (KRA) spectral hardening. The neutrino flux (dot-dashed line) extrapolated from the *Fermi*-LAT diffuse γ flux (purple circles) adapted from [34] up to IceCube energies is shown. The implied flux from the three events from the IceCube 3 years sample [4] is shown as black triangles. The solid black line shows the all-sky average neutrino intensity from the IceCube global fit analysis in the energy range 25 TeV–2.8 PeV [8] integrated over $\Delta\Omega$.

not including the CR hardening (KRA, Fig. 4) yield neutrino fluxes one order of magnitude smaller than that of the extrapolation from *Fermi*-LAT.

6. Conclusions and outlook

An enhanced neutrino production from the central part of the Galactic Plane has been searched for using track-like events observed by the ANTARES telescope from 2007 to 2013. No excess of events has been observed, and limits on the contribution from this possible source to the astrophysical neutrino signal observed by IceCube have been set as a function of spectral index. For a neutrino flux $\propto E^{-2.5}$ we exclude at 90% c.l. that 3 or more events from the 3 year IceCube HESE sample are originating from this region. The extrapolation of the *Fermi*-LAT γ-ray measurement to the IceCube neutrino flux in the Galactic Plane area has also been constrained.

Data taking of the ANTARES neutrino telescope will continue at least up to the end of 2016, increasing the ν_μ statistics available for this analysis. In addition, a new reconstruction procedure for showering events has been developed, with an angular resolution of 3–4 degrees in the TeV–PeV range [45], which can be used to enhance the sensitivity for point-like sources and diffuse emission from small regions of the sky. Preliminary results indicate that using reconstructed cascades, the sensitivity to point sources with $\Gamma = 2$ spectrum improves by about 30%. This suggests that at the end of data taking the sensitivity of ANTARES will reach a level close to the prediction of the model that includes a CR spectral hardening (KRA$_\gamma$) [13].

Acknowledgements

References

[1] M. Ageron, et al., Nucl. Instrum. Methods A 656 (2011) 11.
[2] S. Adrián-Martínez, et al., Astrophys. J. 786 (2014) L5.
[3] M.G. Aartsen, et al., Science 342 (2013) 1242856.
[4] M.G. Aartsen, et al., Phys. Rev. Lett. 113 (2014) 101101.
[5] M.G. Aartsen, et al., Phys. Rev. D 91 (2015) 022001.
[6] M.G. Aartsen, et al., Phys. Rev. Lett. 115 (2015) 081102.
[7] T.K. Gaisser, et al., Phys. Rev. D 90 (2014) 023009.
[8] M.G. Aartsen, et al., Astrophys. J. 809 (2015) 98.
[9] M.G. Aartsen, et al., Phys. Rev. Lett. 114 (2015) 171102.
[10] S. Adrián-Martínez, et al., Astrophys. J. 760 (2012) 53.
[11] S. Adrián-Martínez, et al., arXiv:1511.02149, 2015.
[12] A. Abramowski, et al., Nature 531 (2016) 476–479.
[13] D. Gaggero, et al., Astrophys. J. Lett. 815 (2015) L25.
[14] Y.Q. Guo, H.B. Hu, Z. Tian, arXiv:1412.8590, 2014.
[15] M. Ahlers, K. Murase, Phys. Rev. D 90 (2014) 023010.
[16] M. Alhers, et al., Phys. Rev. D 93 (2016) 013009.
[17] S. Adrián-Martínez, et al., Eur. Phys. J. C 73 (2013) 2606.
[18] J. Schnabel, et al., Nucl. Instrum. Methods A 725 (2013) 106–109.
[19] E. Fermi, Phys. Rev. 75 (1949) 1169.
[20] E. Fermi, Astrophys. J. 119 (1954) 1.
[21] J. Bahcall, E. Waxman, Phys. Rev. D 64 (2001) 023002.
[22] A. Neronov, D. Semikoz, Astropart. Phys. 75 (2016) 60–63.
[23] A. Palladino, F. Vissani, arXiv:1601.06678, 2016.
[24] M. Spurio, Phys. Rev. D 90 (2014) 103004.
[25] E. Waxman, J.N. Bahcall, Phys. Rev. Lett. 78 (1997) 2292.
[26] K. Mannheim, R. Protheroe, J.P. Rachen, Phys. Rev. D 63 (2001) 023003.
[27] A. Loeb, E. Waxman, J. Cosmol. Astropart. Phys. 0605 (2006) 003.
[28] S.R. Kelner, F.A. Aharonian, V.V. Bugayov, Phys. Rev. D 74 (3) (2006) 034018.
[29] M. Ackermann, et al., Astrophys. J. 750 (2012) 3.
[30] J.C. Joshi, W. Winter, N. Gupta, Mon. Not. R. Astron. Soc. 439 (2014) 3414.
[31] M. Kachelriess, S. Ostapchenko, Phys. Rev. D 90 (2014) 083002.
[32] A. Abdo, et al., Astrophys. J. 688 (2008) 1078.
[33] F. Aharonian, et al., Nature 439 (2006) 695.
[34] A. Neronov, D. Semikoz, C. Tchernin, Phys. Rev. D 89 (2014) 103002.
[35] A. Margiotta, et al., Nucl. Instrum. Methods A 725 (2012) 53.
[36] L.A. Fusco, A. Margiotta, et al., Proceedings of the VLVnT 2015, Rome, Italy, 2015.
[37] S. Adrián-Martínez, et al., Eur. Phys. J. C 74 (2014) 2701.
[38] G.C. Hill, K. Rawlins, Astropart. Phys. 19 (2003) 393.
[39] G. Carminati, et al., Comput. Phys. Commun. 179 (12) (2008) 915–923.
[40] M. Honda, et al., Phys. Rev. D 75 (2007) 043006.
[41] R. Enberg, et al., Phys. Rev. D 78 (2008) 043005.
[42] E. Visser, et al., J. Phys. Conf. Ser. 632 (2015) 012043;
E. Visser, Neutrinos from the Milky Way, Doctoral Thesis, Leiden University, http://hdl.handle.net/1887/32966.
[43] M. Ackermann, et al., Astrophys. J. 793 (2014) 64.
[44] G.J. Feldman, R.D. Cousins, Phys. Rev. D 57 (1998) 3873–3889.
[45] T. Michael, et al., Proceedings of the 34th ICRC, The Hague, Netherlands, arXiv:1510.04508, 2015.